

Preclinical Pharmacokinetic, Biodistribution, Toxicology, and Dosimetry Studies of ^{111}In -DTPA-Human Epidermal Growth Factor: An Auger Electron-Emitting Radiotherapeutic Agent for Epidermal Growth Factor Receptor-Positive Breast Cancer

Raymond M. Reilly¹⁻³, Paul Chen¹, Judy Wang¹, Deborah Scollard¹, Ross Cameron⁴, and Katherine A. Vallis⁵⁻⁷

¹Division of Nuclear Medicine, University Health Network, Toronto, Ontario, Canada; ²Department of Medical Imaging, University of Toronto, Toronto, Ontario, Canada; ³Department of Pharmaceutical Sciences, University of Toronto, Toronto, Ontario, Canada; ⁴Department of Laboratory Medicine and Pathobiology, University of Toronto, Toronto, Ontario, Canada; ⁵Department of Radiation Oncology, The Princess Margaret Hospital, Toronto, Ontario, Canada; ⁶Department of Medical Biophysics, University of Toronto, Toronto, Ontario, Canada; and ⁷Department of Radiation Oncology, University of Toronto, Toronto, Ontario, Canada

Our objective was to evaluate the pharmacokinetics, normal tissue distribution, radiation dosimetry, and toxicology of human epidermal growth factor (hEGF) labeled with ^{111}In (^{111}In -diethylenetriaminepentaacetic acid [DTPA]-hEGF) in mice and rabbits. **Methods:** ^{111}In -DTPA-hEGF (3.6 MBq; 1.3 or 13 μg) was administered intravenously to BALB/c mice. The blood concentration-time data were fitted to a 3-compartment model. Acute toxicity was studied with female BALB/c mice at 42 times the maximum planned human dose (MBq/kg) or with New Zealand White rabbits at 1 times the maximum planned human dose (MBq/kg) for a phase I clinical trial. Toxicity was evaluated by monitoring body weight, by determination of hematology and clinical biochemistry parameters, and by morphologic examination of tissues. Radiation dosimetry projections in humans were estimated on the basis of the residence times in mice by use of the OLINDA version 1.0 computer program. **Results:** The largest amounts of radioactivity were taken up by the liver (41.3 ± 7.8 [mean \pm SD] percentage injected dose [%ID] at 1 h after injection and decreasing to 4.9 ± 0.3 %ID at 72 h after injection) and kidneys (18.6 ± 0.8 %ID at 1 h and decreasing to 4.5 ± 0.2 %ID at 72 h after injection). ^{111}In -DTPA-hEGF was cleared rapidly from the blood, with a half-life at α -phase of 2.7–6.2 min and a half-life at β -phase of 24.0–36.3 min. The half-life of the long terminal phase could not be accurately determined. The volume of distribution of the central compartment was 340–375 mL/kg, and the volume of distribution at steady state was 430–685 mL/kg. There was no significant difference in the ratio of body weight at 15 d to pretreatment weight for mice administered ^{111}In -DTPA-hEGF (1.02 ± 0.01) and mice administered unlabeled DTPA-hEGF

(1.01 ± 0.01). Erythrocyte, leukocyte, and platelet counts and serum alanine aminotransferase and creatinine levels remained in the normal ranges. No morphologic changes were observed by light microscopy in any of 19 tissues sampled. Minor morphologic changes in the liver were observed by electron microscopy. The projected whole-body dose in humans was $0.19 \text{ mSv}\cdot\text{MBq}^{-1}$. The projected doses to the liver, kidneys, and lower large intestine were 0.76, 1.82, and $1.12 \text{ mSv}\cdot\text{MBq}^{-1}$, respectively. **Conclusion:** ^{111}In -DTPA-hEGF was safely administered to mice and rabbits at multiples of the maximum dose planned for a phase I trial in breast cancer patients.

Key Words: breast cancer; ^{111}In -DTPA-hEGF; pharmacokinetics; toxicology; radiation dosimetry

J Nucl Med 2006; 47:1023–1031

Human epidermal growth factor (hEGF) labeled with ^{111}In (^{111}In -diethylenetriaminepentaacetic acid [DTPA]-hEGF) is a novel targeted radiotherapeutic agent for epidermal growth factor receptor (EGFR)-positive breast cancer (1). The radio-pharmaceutical relies on receptor-mediated binding, internalization, and nuclear translocation of EGF in breast cancer cells to insert ^{111}In into the nucleus of the cells, where the nanometer-to-micrometer-range Auger electrons are most damaging to DNA, thereby killing the cells. Our group discovered that ^{111}In -DTPA-hEGF was highly radiotoxic to MDA-MB-468 human breast cancer cells overexpressing EGFR (1×10^6 – 2×10^6 receptors per cell), reducing their surviving fraction to less than 3% at only 111–148 mBq per cell (1). It was subsequently found that ^{111}In -DTPA-hEGF was 85- to 300-fold more growth inhibitory on a molar-concentration basis to MDA-MB-468

Received Dec. 9, 2005; revision accepted Feb. 18, 2006.

For correspondence or reprints contact: Raymond M. Reilly, PhD, Leslie Dan Faculty of Pharmacy, University of Toronto, 19 Russell St., Toronto, Ontario M5S 2S2, Canada.

E-mail: raymond.reilly@utoronto.ca

cells than commonly used chemotherapeutic agents for breast cancer, such as doxorubicin, paclitaxel, or methotrexate, and several logarithms more effective than 5-fluorouracil (2). Treatment of athymic mice implanted subcutaneously with MDA-MB-468 breast cancer xenografts with 5 weekly doses of ^{111}In -DTPA-hEGF (18.5 MBq; 3.4 μg) significantly slowed the growth of well-established tumors by 3-fold and caused the regression of small, nonestablished tumors (3).

These promising preclinical results led us to propose a phase I clinical trial of ^{111}In -DTPA-hEGF for the treatment of patients with chemotherapy-resistant, EGFR-positive metastatic breast cancer; this trial is now in progress at the Princess Margaret Hospital in Toronto, Ontario, Canada (4). To translate the preclinical findings to the phase I trial, a kit was formulated under good manufacturing practices for the preparation of ^{111}In -DTPA-hEGF; the details of this kit were recently reported (5). In the present article, we describe the results of preclinical studies examining the pharmacokinetics, normal tissue distribution, toxicology, and radiation dosimetry of ^{111}In -DTPA-hEGF prepared by use of the kit; all of these properties were required for regulatory approval of the clinical trial application by Health Canada.

MATERIALS AND METHODS

Radiopharmaceutical

^{111}In -DTPA-hEGF was prepared by adding ^{111}In -chloride (>1.85 GBq/mL; MDS-Nordion, Inc.) to 250 μg of DTPA-conjugated hEGF₁₋₅₁ in 1 mL of sodium acetate buffer (1 mol/L; pH 6.0) as previously reported (5). The radiochemical purity of ^{111}In -DTPA-hEGF was determined to be greater than 98% by instant thin-layer silica gel chromatography (Pall) with sodium citrate buffer (100 mmol/L; pH 5.0).

Pharmacokinetic Studies

Groups of 6–8 female BALB/c mice were injected intravenously (tail vein) with 3.6 MBq (1.3 μg) of ^{111}In -DTPA-hEGF or with 3.6 MBq (1.3 μg) of ^{111}In -DTPA-hEGF mixed with 11.7 μg of DTPA-hEGF (total, 13 μg). This 10-fold range in mass was studied to determine whether there were nonlinear pharmacokinetics for ^{111}In -DTPA-hEGF at high doses. Blood samples (approximately 25 μL) were collected into calibrated heparinized microcapillary tubes (Fisher Scientific Co.) by femoral vein puncture up to 72 h after injection. The microcapillaries were transferred to γ -counting tubes and subjected to counting along with a standard of the injected dose in a γ -counter (Cobra II series Auto-Gamma System model 5003; Packard Instrument Co.). The concentrations of radioactivity in blood were expressed as percentage injected dose (%ID) per milliliter (%ID/mL). The mean %ID/mL values were plotted against time after injection, and the resulting elimination curves were fitted to a 3-compartment pharmacokinetic model by use of Scientist version 2.01 software (MicroMath Scientific Software). Standard pharmacokinetic parameters were estimated.

Stability in Plasma

The transchelation of radioactivity from ^{111}In -DTPA-hEGF to transferrin in mouse or human plasma in vitro at 37°C for up to 72 h was determined by size exclusion high-pressure liquid chromatography (HPLC) with a BioSep SEC-S2000 column

(Phenomenex) eluted with sodium phosphate buffer (100 mmol/L; pH 6.8) at a flow rate of 0.8 mL/min. Peaks were monitored by use of a flowthrough radioactivity detector (model 170; Beckman-Coulter). An HPLC standard for ^{111}In -transferrin was prepared by incubating ^{111}In -acetate with plasma for 24 h. ^{111}In -DTPA-hEGF diluted in sodium bicarbonate buffer (50 mmol/L; pH 7.5) was used as a negative control.

Biodistribution Studies

Female BALB/c mice were injected intravenously (tail vein) with 0.9–1.1 MBq (0.25–0.3 μg) of ^{111}In -DTPA-hEGF. Groups of 3 mice were sacrificed at selected times up to 72 h after injection. Samples of blood and tissues were obtained, weighed, and subjected to counting along with a standard of the injected dose in a γ -counter. The accumulation of radioactivity in tissues was expressed as %ID per gram (%ID/g) and as %ID per organ (%ID/organ). Standard mouse organ weights previously recorded in our laboratory were used to calculate %ID/organ values from %ID/g values.

Toxicology Studies

Groups of 7 female BALB/c mice were injected intravenously (tail vein) with 44.4 MBq (3–30 μg) of ^{111}In -DTPA-hEGF or an equivalent amount of unlabeled DTPA-hEGF. Groups of 3 pathogen-free female New Zealand White rabbits (nonrodent species) were injected intravenously (marginal ear vein) with 85.1 MBq (58 μg) of ^{111}In -DTPA-hEGF or an equivalent amount of unlabeled DTPA-hEGF. These doses were selected because they were the maximum doses allowed under our internal radiation safety permit at the University Health Network and represented 42 times (mice) or 1 times (rabbits), respectively, the maximum planned dose for the phase I clinical trial of ^{111}In -DTPA-hEGF scaled on an MBq/kg basis. Body weight was monitored for 15 d in mice and for 18 d in rabbits. At the end of the monitoring period, the mice were anesthetized and sacrificed by cervical dislocation, and the rabbits were euthanized with sodium pentobarbital (Euthanyl; Abbott Laboratories). Blood samples (approximately 50 μL) were collected from mice and rabbits into heparinized microcapillary tubes. The samples were pooled to provide sufficient samples for analysis by the core laboratory at the Hospital for Sick Children, Toronto, Ontario, Canada. Hematology analyses included leukocyte (WBC), erythrocyte (RBC), and platelet counts as well as hematocrit (Hct) and hemoglobin (Hb) concentrations. Biochemistry analyses included serum alanine aminotransferase (ALT) and creatinine (Cr) levels. In addition, samples of 19 different tissues were obtained at necropsy, fixed in formalin, embedded in paraffin, and sectioned. All sections were stained with hematoxylin and eosin and examined by light microscopy (LM) by a clinical pathologist. Sections of the liver, kidneys, and cornea (tissues that express EGFR) were further examined in detail by electron microscopy (EM).

Radiation Dosimetry Projections

The area under the curve (AUC) from 0 to 72 h ($\text{Bq} \times \text{h}$) for the radioactivity–time curve derived for each organ (not corrected for radioactive decay) from biodistribution studies was integrated from the time of injection of ^{111}In -DTPA-hEGF to the last sampled time point (72 h after injection) by use of the trapezoidal rule (6). The AUC from 72 h after injection to infinity was estimated by dividing the amount of radioactivity (Bq) at the 72-h time point by the physical decay constant for ^{111}In ($1.03 \times 10^{-2} \text{h}^{-1}$), thus assuming elimination only by radioactive decay. The mean

residence time of radioactivity in each organ (h) was calculated by dividing the total AUC from 0 h to infinity ($\text{Bq} \times \text{h}$) by the injected dose (Bq). The radiation-absorbed doses in humans ($\text{mSv} \cdot \text{Bq}^{-1}$) were projected on the basis of the organ and whole-body residence times in mice and were estimated by use of the OLINDA version 1.0 computer program (7). For projection of the radiation-absorbed doses to the eyes, the sphere model in the OLINDA program was used, assuming a mass of 8 g for each eye. The radionuclide contaminants $^{114\text{m}}\text{In}$ and ^{65}Zn , present at less than 0.1% in ^{111}In -chloride, were taken into consideration in estimating the total radiation-absorbed doses.

Ethical Approval

The principles of laboratory animal care (8) were followed. Animal studies were conducted under a protocol approved by the Animal Care Committee at the University Health Network (UHN-03-003) and in accordance with Canadian Council on Animal Care guidelines.

RESULTS

Pharmacokinetic Studies

The mean concentrations of radioactivity (%ID/mL) in the blood over time for groups of 6–8 BALB/c mice after intravenous (tail vein) administration of a low mass ($1.3 \mu\text{g}$) or a high mass ($13 \mu\text{g}$) of ^{111}In -DTPA-hEGF (3.6 MBq) are shown in Figure 1. The higher dose of ^{111}In -DTPA-hEGF was distributed more rapidly than the lower dose (half-life at α -phase [$t_{1/2\alpha}$], 2.7 vs. 6.2 min, respectively). However, the higher dose of ^{111}In -DTPA-hEGF was cleared more slowly than the lower dose (half-life at β -phase [$t_{1/2\beta}$], 24.0 vs. 36.3 min, respectively). In both cases, ^{111}In -DTPA-hEGF exhibited a very long terminal elimination phase. The half-life of this final phase could not be accurately estimated because of the limited number of data points in this phase. The volume of distribution of the central compartment (V_1) for ^{111}In -DTPA-hEGF was 6.8 mL (340 mL/kg) for the low dose and 7.5 mL (375 mL/kg) for the high dose. The volume of distribution at steady state (V_{ss}) was 13.7 mL (685 mL/kg) for the low dose and 8.6 mL (430 mL/kg) for the high dose. The V_1 was about 5 or 6 times larger than the expected plasma volume (V_p) (9), and the V_{ss} (430 – 685 mL/kg) was 7–10 times larger than the V_p . The systemic clearance for ^{111}In -DTPA-hEGF was 0.41 mL/min (20.5 mL/min/kg) for the low dose and 0.25 mL/min (12.5 mL/min/kg) for the high dose.

Biodistribution Studies

The accumulation of radioactivity in tissues of BALB/c mice up to 72 h after injection of ^{111}In -DTPA-hEGF (0.9 – 1.1 MBq ; 0.25 – $0.3 \mu\text{g}$) is shown in Figure 2. The kidneys and liver accumulated the highest concentrations (%ID/g) of ^{111}In . However, radioactivity in the kidneys decreased from 51.8 ± 2.4 (mean \pm SD) %ID/g at 1 h after injection to 12.5 ± 0.7 %ID/g at 72 h after injection, and liver radioactivity decreased from 29.7 ± 5.6 %ID/g at 1 h after injection to 3.6 ± 0.2 %ID/g at 72 h after injection. Consistent with the pharmacokinetic studies, the concentrations

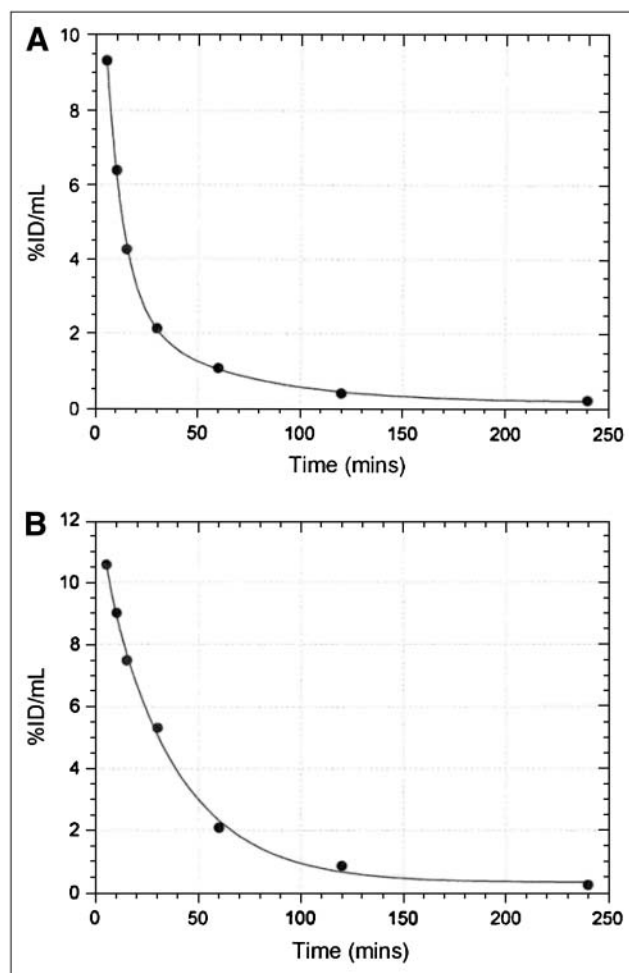


FIGURE 1. Elimination of radioactivity from blood of 6–8 BALB/c mice injected intravenously (tail vein) with ^{111}In -DTPA-hEGF. %ID/mL–time curves were fitted to 3-compartment pharmacokinetic model. (A) Mice injected with low mass of ^{111}In -DTPA-hEGF (3.6 MBq; $1.3 \mu\text{g}$). (B) Mice injected with high mass of ^{111}In -DTPA-hEGF (3.6 MBq; $13.0 \mu\text{g}$).

of radioactivity in the blood decreased rapidly from 0.9 ± 0.2 %ID/g at 1 h after injection to only 0.04 ± 0.01 %ID/g at 72 h after injection. The liver accumulated the highest proportion of the injected dose (41.3 ± 7.8 %ID at 1 h after injection), but this value decreased to 7.3 ± 0.4 %ID at 72 h after injection. The kidneys accumulated 18.6 ± 0.8 %ID at 1 h after injection; this value decreased to 6.4 ± 0.7 %ID at 72 h after injection. The eyes accumulated 0.1 ± 0.02 %ID at 1 h after injection; this value decreased to 0.04 ± 0.01 %ID at 72 h after injection. Although the concentration (%ID/g) of radioactivity in the intestines and bone was low (Fig. 2A), these organs sequestered high proportions of the injected dose (Fig. 2B) because of their relatively large masses (3.8 and 3.6 g, respectively). The intestines and bone accumulated 27.1 ± 2.9 and 10.4 ± 0.7 %ID, respectively, at 1 h after injection; these values decreased to 0.6 ± 0.04 and 1.04 ± 0.3 %ID at 72 h after injection.

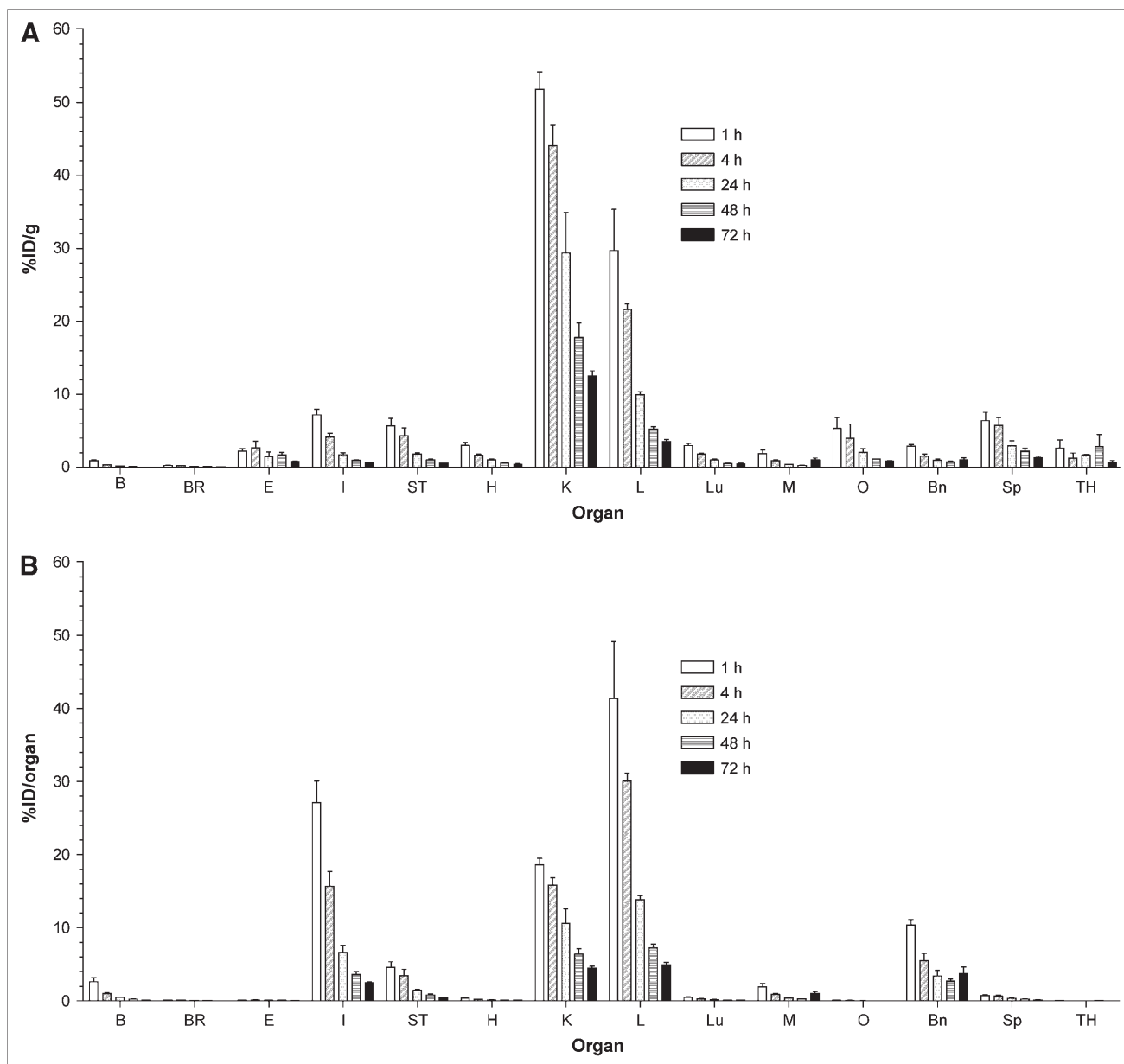


FIGURE 2. Tissue distribution of radioactivity at selected times after intravenous (tail vein) injection of ^{111}In -DTPA-hEGF (0.9–1.1 MBq; 0.25–0.3 μg) in BALB/c mice. (A) Tissue uptake expressed as %ID/g. (B) Tissue uptake expressed as %ID/organ. Error bars are SEM of 3 mice. B = blood; BR = brain; E = eyes; I = intestines; ST = stomach; H = heart; K = kidneys; L = liver; Lu = lungs; M = muscle; O = ovaries; Bn = bone; Sp = spleen; TH = thyroid.

Stability in Plasma

Representative HPLC results for ^{111}In -DTPA-hEGF diluted with sodium bicarbonate buffer (50 mmol/L; pH 7.5) or incubated with mouse plasma for 24 h are shown in Figures 3A and 3B. Similar results (not shown) were obtained for human plasma. Over a 72-h period, 27%–33% of ^{111}In was transchelated from ^{111}In -DTPA-hEGF in vitro to transferrin (9%–11%/d).

Toxicology Studies

There was no significant decrease in the body weights of female BALB/c mice administered 44.4 MBq (3–30 μg)

of ^{111}In -DTPA-hEGF or an equivalent amount of unlabeled DTPA-hEGF over a 15-d period (Table 1). Similarly, there was no significant decrease in the body weights of female New Zealand White rabbits administered 85.1 MBq (58 μg) of ^{111}In -DTPA-hEGF or an equivalent amount of unlabeled DTPA-hEGF over an 18-d period (Table 2). There were also no signs of dehydration, lethargy, or ataxia in either group of mice. These results indicated that there was no generalized normal tissue toxicity associated with ^{111}In -DTPA-hEGF or unlabeled DTPA-hEGF.

Biochemistry and hematology results obtained for BALB/c mice at 15 d after injection of ^{111}In -DTPA-hEGF

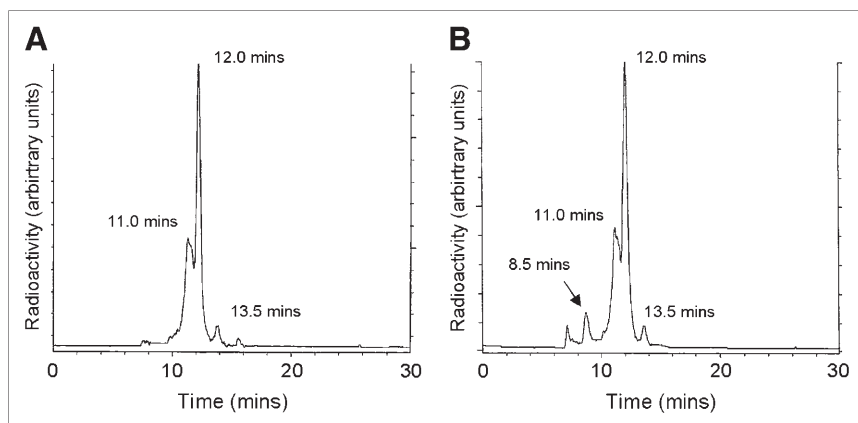


FIGURE 3. HPLC of ^{111}In -DTPA-hEGF. BioSep SEC-S2000 column was eluted with sodium phosphate buffer (100 mmol/L; pH 6.8) at flow rate of 0.8 mL/min. Monitoring was done with Beckman-Coulter model 170 radioactivity detector. (A) ^{111}In -DTPA-hEGF diluted in sodium bicarbonate buffer (50 mmol/L; pH 7.5). Peaks with retention times of 11.0 and 12.0 min correspond to dimerized and monomeric ^{111}In -DTPA-hEGF, respectively. Peak with retention time of 13.5 min represents small amount (<2%) of ^{111}In -DTPA

impurity. (B) ^{111}In -DTPA-hEGF incubated in mouse plasma for 24 h at 37°C. Peak with retention time of 8.5 min represents ^{111}In that has been transchelated from ^{111}In -DTPA-hEGF to transferrin (9%).

(44.4 MBq) or an equivalent amount of unlabeled DTPA-hEGF are shown in Table 3. WBC, RBC, Hb, Hct, and platelet counts and serum ALT levels in mice administered ^{111}In -DTPA-hEGF all remained within or close to the expected normal ranges (10). Serum Cr levels in mice administered ^{111}In -DTPA-hEGF or DTPA-hEGF were lower than the expected normal ranges, but this result may be explained by the young age of the mice (3–4 wk old). Importantly, there was no elevation in serum Cr levels, which would suggest renal toxicity. Platelet counts in mice administered unlabeled DTPA-hEGF could not be determined because of insufficient quality of the sample. Nevertheless, this group of mice received the same mass of DTPA-hEGF as those administered ^{111}In -DTPA-hEGF (which did not show a decrease in platelet counts). The results of analogous biochemistry and hematology studies with New Zealand White rabbits at 18 d after injection of ^{111}In -DTPA-hEGF (85.1 MBq) or an equivalent amount of unlabeled DTPA-hEGF (Table 4) showed that all biochemical and hematologic parameters (including platelet counts) remained within the normal ranges, except for serum Cr levels, which were slightly lower than those for an untreated rabbit.

In mice administered ^{111}In -DTPA-hEGF or unlabeled DTPA-hEGF, there was no evidence of morphologic damage detected by LM in the brain, eyes (including cornea), lungs, heart, thyroid, stomach, ileum (small intestine), cecum (large intestine), pancreas, liver, kidneys, adrenal glands, ovaries, uterus, mammary glands, spleen, bone marrow, muscle, and nerve tissue (results not shown). Similarly, no changes were detected by LM in any of these tissues in rabbits administered ^{111}In -DTPA-hEGF or unlabeled DTPA-hEGF. There were some minor morphologic changes (“ballooning” of smooth endoplasmic reticulum and vacuolization of hepatocytes) in the EM studies of the liver in all rabbits administered ^{111}In -DTPA-hEGF (Fig. 4A). No morphologic abnormalities were detected by EM studies of the kidneys (Fig. 4B) or corneas (Fig. 4C) in rabbits receiving ^{111}In -DTPA-hEGF or unlabeled DTPA-hEGF.

Radiation Dosimetry Projections

The radiation-absorbed dose projections for the administration of ^{111}In -DTPA-hEGF to humans, determined from the residence times in mice, are shown in Table 5. It was expected that the highest absorbed doses would be received

TABLE 1

Body Weights of BALB/c Mice Administered ^{111}In -DTPA-hEGF or Unlabeled DTPA-hEGF*

Time after injection (d)	Normalized body weight after administration of†:	
	^{111}In -DTPA-hEGF	DTPA-hEGF
3	1.01 ± 0.01	1.03 ± 0.02
7	1.02 ± 0.01	1.02 ± 0.01
10	1.04 ± 0.02	1.02 ± 0.01
13	1.00 ± 0.02	1.01 ± 0.01
15	1.02 ± 0.01	1.01 ± 0.01

*Mice were intravenously administered 44.4 MBq (3–30 μg) of ^{111}In -DTPA-hEGF or equivalent amount of unlabeled DTPA-hEGF.

†Body weight is expressed as mean ± SEM of fraction of initial body weight (on day 0) for groups of 3 mice.

TABLE 2

Body Weights of New Zealand White Rabbits Administered ^{111}In -DTPA-hEGF or Unlabeled DTPA-hEGF*

Time after injection (d)	Normalized body weight after administration of†:	
	^{111}In -DTPA-hEGF	DTPA-hEGF
3	1.07 ± 0.01	1.03 ± 0.01
6	1.08 ± 0.03	1.03 ± 0.01
10	1.14 ± 0.01	1.11 ± 0.05
14	1.16 ± 0.02	1.12 ± 0.03
18	1.12 ± 0.01	1.08 ± 0.02

*Rabbits were intravenously administered 85.1 MBq (58 μg) of ^{111}In -DTPA-hEGF or equivalent amount of unlabeled DTPA-hEGF.

†Body weight is expressed as mean ± SEM of fraction of initial body weight (on day 0) for groups of 3 rabbits.

TABLE 3

Results of Biochemistry and Hematology Analyses at 15 Days After Injection of ^{111}In -DTPA-hEGF or Unlabeled DTPA-hEGF into BALB/c Mice

Parameter	Mean value after injection of*:		Normal range†
	^{111}In -DTPA-hEGF	DTPA-hEGF	
WBC ($10^9/\text{L}$)	6.4	7.4	5.0–13.7
RBC ($10^{12}/\text{L}$)	8.1	9.2	7.9–10.1
Hb (g/L)	137	153	110–145
Hct	0.398	0.451	0.400
Platelets ($10^9/\text{L}$)	521	ND	600–1,200
ALT (U/L)	23	36	28–184
Cr ($\mu\text{mol/L}$)	33	51	119–155

*Mean value for blood or serum samples pooled from 7 mice administered 44.4 MBq (3–30 μg) of ^{111}In -DTPA-hEGF or equivalent amount of unlabeled DTPA-hEGF. ND = not determined because of subquality of sample obtained.

†Expected normal range was obtained from Olfert et al. (10).

by the kidneys ($1.82 \text{ mSv}\cdot\text{MBq}^{-1}$), lower large intestine ($1.12 \text{ mSv}\cdot\text{MBq}^{-1}$), and liver ($0.76 \text{ mSv}\cdot\text{MBq}^{-1}$), whereas the whole-body radiation-absorbed dose would be $0.19 \text{ mSv}\cdot\text{MBq}^{-1}$. The red marrow absorbed dose estimated by the OLINDA program on the basis of the uptake of ^{111}In -DTPA-hEGF in bone would be $0.20 \text{ mSv}\cdot\text{MBq}^{-1}$. The radiation-absorbed doses to the thyroid and eyes would be 0.13 and $0.15 \text{ mSv}\cdot\text{MBq}^{-1}$, respectively.

DISCUSSION

In this report, we describe for the first time detailed preclinical studies that reveal the pharmacokinetics, tissue

TABLE 4

Results of Biochemistry and Hematology Analyses at 18 Days After Injection of ^{111}In -DTPA-hEGF or Unlabeled DTPA-hEGF into New Zealand White Rabbits

Parameter	Mean value after injection of*:		Normal range†
	^{111}In -DTPA-hEGF	DTPA-hEGF	
WBC ($10^9/\text{L}$)	6.7	7.7	4.0–13.0
RBC ($10^{12}/\text{L}$)	5.6	5.7	4.5–8.5
Hb (g/L)	119	118	94–175
Hct	0.354	0.367	0.365
Platelets ($10^9/\text{L}$)	330	275	180–750
ALT (U/L)	79	44	10–80
Cr ($\mu\text{mol/L}$)	70	64	113‡

*Mean value for blood or serum samples from 3 rabbits administered 85.1 MBq (58 μg) of ^{111}In -DTPA-hEGF or equivalent amount of unlabeled DTPA-hEGF.

†Expected normal range was obtained from Olfert et al. (10).

‡No normal range available; value was obtained from untreated control rabbit.

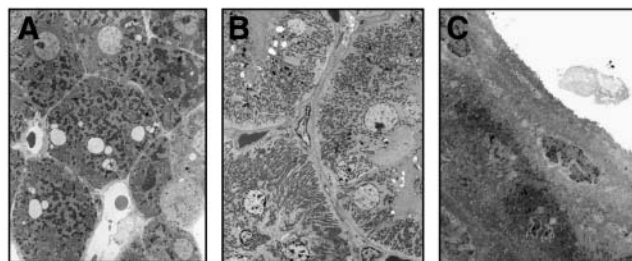


FIGURE 4. EM of tissues from representative New Zealand White rabbit at 18 d after intravenous (marginal ear vein) injection of ^{111}In -DTPA-hEGF (85.1 MBq; 58 μg). (A) Liver. (B) Kidneys. (C) Cornea. Slight ballooning of smooth endoplasmic reticulum and vacuolization of hepatocytes in liver were seen. No morphologic abnormalities were detected in kidneys or cornea.

biodistribution, toxicology, and radiation dosimetry of ^{111}In -DTPA-hEGF prepared from a kit (5) for study in a phase I clinical trial in breast cancer patients. These preclinical studies were required by Health Canada for approval of the clinical trial application. ^{111}In -DTPA-hEGF was eliminated very rapidly from the blood after intravenous (tail vein) injection in BALB/c mice. The blood concentration–time curve was best described by a 3-compartment pharmacokinetic model. The $t_{1/2\alpha}$ of 2.7–6.2 min was longer than that previously reported by Kurihara et al. (11) for ^{111}In -DTPA-hEGF administered intravenously to rats ($t_{1/2\alpha} = 0.7 \text{ min}$). The $t_{1/2\beta}$ of 24.0–36.3 min for ^{111}In -DTPA-hEGF in BALB/c mice was

TABLE 5

Radiation-Absorbed Dose Projections for ^{111}In -DTPA-hEGF in Humans

Organ	Radiation-absorbed dose ($\text{mSv}\cdot\text{MBq}^{-1}$)*
Brain	0.06
Lower large intestine	1.12
Stomach	0.39
Heart	0.20
Kidneys	1.82
Liver	0.76
Lungs	0.16
Muscle	0.14
Ovaries	0.39
Osteogenic cells	0.52
Red marrow	0.20
Spleen	0.34
Thyroid	0.13
Eyes	0.15
Whole body	0.19

*Radiation-absorbed dose projections in humans were determined from residence times for ^{111}In -DTPA-hEGF in BALB/c mice and were calculated by use of OLINDA version 1.0 computer program. Maximum of 0.1% of each of radionuclide impurities ($^{114\text{m}}\text{In}$ and ^{65}Zn) in ^{111}In was considered in estimating total radiation-absorbed doses.

similar to that in rats ($t_{1/2\beta} = 33$ min). In the present study, the $t_{1/2\beta}$ in mice administered a high dose (13 μ g; 650 μ g/kg) of the radiopharmaceutical was longer than that in mice administered a 10-fold-lower dose (36.3 vs. 24.0 min, respectively). This finding may be attributable to partial saturation of the hepatic transport mechanism (12). St. Hilaire et al. (13) found that combining 125 I-EGF with a 100-fold excess of unlabeled EGF decreased liver sequestration from 99% to 24% after portal administration of the peptide to rats. Kurihara et al. (11) did not report the V_1 for 111 In-DTPA-hEGF in rats, but the V_{ss} (1,297 mL/kg) was about 2 or 3 times larger than that which we observed in mice (430–685 mL/kg). The V_1 and V_{ss} for 111 In-DTPA-hEGF in mice were 5- to 6-fold and 7–10 times larger, respectively, than the V_p (65 mL/kg) (9). These large volumes of distribution for 111 In-DTPA-hEGF likely reflected the high proportions of sequestration of the radiopharmaceutical by the liver and kidneys, as noted in the biodistribution studies.

Biodistribution studies with BALB/c mice administered 111 In-DTPA-hEGF revealed that a large proportion of the injected dose (%ID/organ) was rapidly accumulated by the liver and kidneys, but the amount of radioactivity in these organs decreased 6- and 3-fold, respectively, over a 72-h period. The concentration of radioactivity in the kidneys was higher than that in the liver (12.5 ± 0.7 vs. 3.6 ± 0.2 %ID/g, respectively). These values were similar to those previously reported for kidney and liver uptake of 111 In-DTPA-hEGF (14) in athymic mice and likely were attributable to the moderate levels of EGFR expressed by these tissues (12,15). Although it is difficult to compare directly the tissue distributions of peptides conjugated to radiometals and those labeled with radioiodine because of their different metabolic routes, the overall pattern of biodistribution of 111 In-DTPA-hEGF in BALB/c mice was analogous to that reported for 125 I-EGF in rats (16). Renal excretion likely contributes to the kidney uptake of 111 In-DTPA-hEGF, because 125 I-EGF is filtered by the glomerulus and secreted but not reabsorbed by renal tubules in rabbits (17). Renal uptake of radioactivity was not attributable to the excretion of 111 In-DTPA impurities present in 111 In-DTPA-hEGF, because the radiochemical purity was greater than 98%. Transchelation of 111 In from 111 In-DTPA-hEGF to transferrin occurred at a rate of 9%–11%/d in vitro in mouse or human plasma. This rate of transchelation was similar to that previously reported for 111 In-DTPA-conjugated antibodies (18). Transchelation of 111 In from 111 In-DTPA-hEGF to transferrin may contribute to hepatic and bone marrow uptake of radioactivity. The thyroid expresses EGFR (19), but radioactivity in the thyroid of mice administered 111 In-DTPA-hEGF in the present study was only 0.03 ± 0.01 %ID at 1 h after injection and decreased to 0.01 ± 0.002 %ID at 72 h after injection. Similarly, corneal tissue is EGFR positive (20), but radioactivity in the eyes of mice was only 0.10 ± 0.02 %ID at 1 h after injection and decreased to 0.04 ± 0.01 %ID

at 72 h after injection of 111 In-DTPA-hEGF in the present study.

There were no hematologic, hepatic, kidney, or other normal tissue toxicities associated with the administration of 111 In-DTPA-hEGF to female BALB/c mice at doses (44.4 MBq; 3–30 μ g) equivalent to 42 times the maximum planned human radioactivity dose (2,960 MBq; 0.25 mg) for a phase I clinical trial on an MBq/kg basis. Similarly, there were no toxicities associated with 111 In-DTPA-hEGF (85.1 MBq; 58 μ g) administered to female New Zealand White rabbits (nonrodent species) at doses equivalent to 1 times the maximum planned human dose on an MBq/kg basis. Bone marrow toxicity caused by the Auger electron emissions of 111 In was not anticipated for 2 reasons: there is no “cross-fire” effect from the Auger electrons, and less than 3% of the hematopoietic stem cell population expresses EGFR (21). Receptor-mediated internalization and nuclear translocation are required for the Auger electrons emitted by 111 In-DTPA-hEGF to manifest their toxic effects (1). Nevertheless, this fact does not preclude radiotoxicity from the low-linear-energy-transfer γ -emissions of 111 In, especially at the higher dose to be administered in the phase I clinical trial. Importantly, there was no evidence of major toxicity to the liver or kidneys in mice or rabbits; these tissues have moderate levels of EGFR expression (12,15), and they accumulated large amounts of 111 In-DTPA-hEGF in mice. Minor morphologic changes (ballooning of smooth endoplasmic reticulum and vacuolization of hepatocytes) were noted by EM in the liver of rabbits, but these findings were not associated with elevations in ALT levels and therefore were not considered important by the clinical pathologist. No morphologic changes were observed in rabbits administered unlabeled DTPA-hEGF, suggesting an effect that may be mediated by the radiation effects of 111 In, most likely the Auger electrons. Because morphologic changes were not observed in BALB/c mice administered a single dose of 44 MBq of 111 In-DTPA-hEGF or in an earlier study (1) in which athymic mice were administered 2 doses (37 and 74 MBq) of 111 In-DTPA-hEGF, this finding suggests that they were species dependent. Differences in the mechanisms of hepatobiliary clearance of drugs between rabbits and rodents may explain these observations for 111 In-DTPA-hEGF (22). EGFR is expressed in corneal tissue (20), but we did not detect any morphologic damage to this tissue over a 15-d period in mice or an 18-d period in rabbits. A longer observation interval may be required to evaluate this potential risk fully. Radiation dosimetry projections for the eyes in humans revealed that 444 mSv (44.4 cGy) would be absorbed at the maximum dose of 2,960 MBq planned for the phase I clinical trial. This radiation-absorbed dose is 45 times lower than the lowest dose of external radiation that caused cataract formation in humans (2,000 cGy) and is 5- to 6-fold lower than the absorbed dose associated with the formation of opacities (250 cGy) (23). The latency period for the formation of ocular toxicities is approximately 8 y from exposure to external radiation.

Health Canada requires a minimum 7-d observation period to evaluate the acute toxicity of an investigational new drug proposed for administration in a single dose in a phase I clinical trial (24). A longer period of time may be required to evaluate fully hepatic and renal toxicities from ^{111}In -DTPA-hEGF, but the results of the present study were consistent with those of an earlier study in which BALB/c mice were administered a total of 111 MBq of ^{111}In -DTPA-hEGF (37 MBq initially, followed by 74 MBq 4 wk later) and observed for a longer period of 7 wk (1). In that earlier study, no changes in serum Cr or ALT levels or in body weights were observed for mice receiving ^{111}In -DTPA-hEGF. Furthermore, in another study (3), mice were administered a cumulative dose of up to 92.5 MBq of ^{111}In -DTPA-hEGF in 5 weekly amounts. No decreases in body weight or increases in serum ALT or Cr levels were detected, and no evidence of damage to the liver or kidneys was observed over 7 wk. There was, however, a 1.4- to 2-fold decrease in platelet and WBC counts, a result that was thought to be attributable to irradiation and killing of some bone marrow stem cells by the low-linear-energy-transfer γ -emissions of ^{111}In at the very high dose used (80 times the maximum planned human dose for the phase I trial on an MBq/kg basis).

The paradoxical toxicity of ^{111}In -DTPA-hEGF toward breast cancer cells expressing high levels of EGFR but not against the liver or kidneys, tissues that express moderate levels of EGFR, may be attributable to differences in its subcellular distribution. It was recently reported that the EGF-EGFR complex may play a novel role as a nuclear transcription factor for the cyclin D1 gene, particularly in rapidly dividing cells, for example, cancer cells (25). In normal epithelial cells, EGF acts mainly by activating signaling cascades; it is internalized into cytoplasmic vesicles and degraded. In contrast, in cancerous epithelial cells, some internalized EGF molecules circumvent the lysosomal degradation pathway and translocate to the nucleus, a process possibly mediated by a nuclear localization sequence (RRRHIVRKRTLRR) at residues 645–657 in EGFR (26). The radiation-absorbed dose deposited in the nucleus is about 15 times higher when ^{111}In decays in the nucleus than when it decays in the cytoplasm and 30 times higher with decay in the nucleus than with decay on the cell surface (27); this differential nuclear uptake may provide a second level of selectivity that protects EGFR-positive normal cells, in addition to the fact that they express EGFR at lower levels than do malignant cells.

The whole-body radiation-absorbed dose projected for the administration of ^{111}In -DTPA-hEGF to humans ($0.19 \text{ mSv}\cdot\text{MBq}^{-1}$) is 1.5-fold higher than that for ^{111}In -pentetreotide ($0.12 \text{ mSv}\cdot\text{MBq}^{-1}$) (28), the only ^{111}In -labeled peptide receptor-targeted radiotherapeutic agent to be examined clinically (29,30). The kidneys would receive the highest radiation-absorbed dose from ^{111}In -DTPA-hEGF ($1.82 \text{ mSv}\cdot\text{MBq}^{-1}$). At a maximum planned dose of 2,960 MBq, the total radiation-absorbed dose to the

kidneys would be $5.4 \times 10^3 \text{ mSv}$ (540 cGy). This dose is one fourth the maximum tolerated dose for the kidneys, as determined by external radiation data (2,300–2,500 cGy) (31). Moreover, for Auger electron-emitting radiotherapeutic agents such as ^{111}In -DTPA-hEGF, microdosimetry is very important, because it was found that high doses of ^{111}In -pentetreotide that deposited more than 4,500 cGy in the kidneys did not cause renal toxicity in humans (29,30). This finding is in contrast to the clinical experience with ^{90}Y -labeled analogs, for example, ^{90}Y -DOTATOC (32). Unfortunately, currently available information on the subcellular distribution of ^{111}In -DTPA-hEGF in normal tissues is insufficient to estimate microdosimetry. The red marrow dose from ^{111}In -DTPA-hEGF at a maximum administered dose of 2,960 MBq is projected to be 592 mSv (59.2 cGy). This dose is at least one fourth the radiation-absorbed dose previously reported to cause serious myelosuppression with other targeted radiotherapeutic agents (33).

CONCLUSION

We conclude that ^{111}In -DTPA-hEGF was rapidly eliminated from the blood after intravenous administration to BALB/c mice. It localized mainly in the liver, kidneys, and intestines. There was no major toxicity to normal tissues in female BALB/c mice at 42 times the maximum planned dose for a phase I clinical trial in breast cancer patients on an MBq/kg basis. Similarly, there was no significant normal tissue toxicity in female New Zealand White rabbits at 1 times the maximum planned dose in humans on an MBq/kg basis. Projected radiation dosimetry for humans, determined from the biodistribution data in mice, revealed that the radiation-absorbed doses to the whole body and critical organs, for example, kidneys and bone marrow, would be within an acceptable and safe range at the dose of radioactivity planned for the trial.

ACKNOWLEDGMENTS

This research was supported by grants from the U.S. Army Breast Cancer Research Program (DAMD17-02-1-0559), the Susan G. Komen Breast Cancer Foundation (BCTR0100840), and the Ontario Research and Development Challenge Fund. The authors acknowledge the assistance and advice provided by Dr. K. Sandy Pang, Department of Pharmaceutical Sciences, University of Toronto, regarding the fitting of the pharmacokinetic data.

REFERENCES

1. Reilly RM, Kiarash R, Cameron RG, et al. ^{111}In -Labeled EGF is selectively radiotoxic to human breast cancer cells overexpressing EGFR. *J Nucl Med*. 2000;41:429–438.
2. Chen P, Mrkobrada M, Vallis KA, et al. Comparative antiproliferative effects of novel targeted Auger electron radiotherapy, chemotherapy and external γ -radiation on EGFR-overexpressing breast cancer cells. *Nucl Med Biol*. 2002; 29:693–699.
3. Chen P, Cameron R, Wang J, Vallis KA, Reilly RM. Antitumor effects and normal tissue toxicity of ^{111}In -labeled epidermal growth factor administered to

- athymic mice bearing epidermal growth factor receptor-positive human breast cancer xenografts. *J Nucl Med.* 2003;44:1469–1478.
4. Vallis KA, Reilly RM, Scollard DA, et al. A phase I clinical trial of ^{111}In -human epidermal growth factor (^{111}In -hEGF) in patients with metastatic EGFR-positive breast cancer [abstract]. *J Nucl Med.* 2005;46(suppl):152P.
5. Reilly RM, Scollard DA, Wang J, et al. A kit formulated under good manufacturing practices for labeling human epidermal growth factor with ^{111}In for radiotherapeutic applications. *J Nucl Med.* 2004;45:701–708.
6. Gibaldi M, Perrier D. *Pharmacokinetics*. 2nd ed. New York, NY: Marcel Dekker Inc.; 1982:445–449.
7. Stabin MG, Sparks RB, Crowe E. OLINDA/EXM: the second-generation personal computer software for internal dose assessment in nuclear medicine. *J Nucl Med.* 2005;46:1023–1027.
8. *Guide for the Care and Use of Laboratory Animals*. NIH publication no. 86-23. Bethesda, MD: National Institutes of Health; 1985.
9. Sassen A, Reuter AM, Kennes F. Determination of plasma volume in the mouse with screened iodine-labelled proteins. *Experientia.* 1968;24:1203–1204.
10. Olfert ED, Cross BM, McWilliam AA, eds. *Guide to the Care and Use of Experimental Animals*. Ottawa, Ontario, Canada: Canadian Council on Animal Care; 1993:173–176.
11. Kurihara A, Deguchi Y, Pardridge WM. Epidermal growth factor radiopharmaceuticals: ^{111}In chelation, conjugation to a blood-brain barrier delivery vector via a biotin-polyethylene linker, pharmacokinetics, and in vivo imaging of experimental brain tumors. *Bioconj Chem.* 1999;10:502–511.
12. Dunn WA, Hubbard AL. Receptor-mediated endocytosis of epidermal growth factor by hepatocytes in the perfused rat liver: ligand and receptor dynamics. *J Cell Biol.* 1984;98:2148–2159.
13. St. Hilaire RJ, Hradek GT, Jones AL. Hepatic sequestration and biliary secretion of epidermal growth factor: evidence for a high-capacity uptake system. *Proc Natl Acad Sci U S A.* 1983;80:3797–3801.
14. Reilly RM, Kiarash R, Sandhu J, et al. A comparison of EGF and MAb 528 labeled with ^{111}In for imaging human breast cancer. *J Nucl Med.* 2000;41:903–911.
15. Fisher DA, Salido EC, Barajas L. Epidermal growth factor and the kidney. *Annu Rev Physiol.* 1989;51:67–80.
16. Jorgensen PE, Poulson SS, Nexø E. Distribution of i.v. administered epidermal growth factor in the rat. *Regul Pept.* 1988;23:161–169.
17. Nielsen S, Nexø E, Christensen EI. Absorption of epidermal growth factor and insulin in rabbit renal proximal tubules. *Am J Physiol.* 1989;256:E55–E63.
18. Reilly R, Marks A, Law J, Lee NS, Houle S. In vitro stability of EDTA and DTPA immunoconjugates of monoclonal antibody 2G3 labelled with In-111. *Appl Radiat Isot.* 1992;43:961–967.
19. Marti U, Ruchti C, Kämpf J, et al. Nuclear localization of epidermal growth factor and epidermal growth factor receptors in human thyroid tissues. *Thyroid.* 2001;11:137–145.
20. Read LC, George-Nascimento C. Epidermal growth factor: physiological roles and therapeutic applications. *Biotechnol Ther.* 1990;1:237–272.
21. Walz TM, Malm C, Nishikawa BK, Wasteson A. Transforming growth factor-alpha (TGF-alpha) in human bone marrow: demonstration of TGF-alpha in erythroblasts and eosinophilic precursor cells and of epidermal growth factor receptors in blastlike cells of myelomonocytic origin. *Blood.* 1995;85:2385–2392.
22. Mahmood I, Sahajwalla C. Interspecies scaling of biliary excreted drugs. *J Pharm Sci.* 2002;91:1908–1914.
23. Merriam GR, Worgul BV. Experimental radiation cataract: its clinical significance. *Bull N Y Acad Med.* 1983;59:372–392.
24. *Health Canada Drugs Directorate Guidelines for Toxicologic Evaluation: Acute Toxicity*. Ottawa, Ontario, Canada: Minister of Supply and Services; 1995.
25. Lin SY, Makino K, Xia W, et al. Nuclear localization of EGF receptor and its potential new role as a transcription factor. *Nat Cell Biol.* 2001;3:802–808.
26. Laduron PM. Genomic pharmacology: more intracellular sites for drug action. *Biochem Pharmacol.* 1992;44:1233–1242.
27. Goddu SM, Howell RW, Rao DV. Cellular dosimetry: absorbed fractions for monoenergetic electron and alpha particle sources and S-values for radionuclides uniformly distributed in different cell compartments. *J Nucl Med.* 1994;35:303–316.
28. Octreoscan kit for the preparation of indium-111 pentetreotide [product monograph]. St. Louis, MO: Mallinckrodt Medical Inc.; 1995.
29. Krenning EP, Valkema R, Kooij PPM, et al. Peptide receptor radionuclide therapy with [indium-111-DTPA-D-Phe]-octreotide. *J Nucl Med.* 1997;38(suppl):47P.
30. Krenning EP, Kooij PPM, Bakker WH, et al. Radiotherapy with a radiolabeled somatostatin analogue, [^{111}In -DTPA-D-Phe 1]-octreotide: a case history. *Ann N Y Acad Sci.* 1994;733:496–506.
31. Cassady JR. Clinical radiation nephropathy. *Int J Radiat Oncol Biol Phys.* 1995;31:1249–1256.
32. Schumacher T, Waldherr C, Mueller-Brand J, Maecke H. Kidney failure after treatment with ^{90}Y -DOTATOC [letter]. *Eur J Nucl Med.* 2002;29:435.
33. Reilly RM. Biomolecules as targeting vehicles for in situ radiotherapy of malignancies. In: Knaeblein J, ed. *Modern Biopharmaceuticals: Design, Development and Optimization*. Weinheim, Germany: Wiley-VCH; 2005:497–526.